

# Microscopic modeling of the relaxation phenomenon using a macroscopic lane-changing model

Jorge A. Laval<sup>a,b,\*</sup> and Ludovic Leclercq<sup>b</sup>

<sup>a</sup>*School of Civil and Environmental Engineering, Georgia Institute of Technology*

<sup>b</sup>*Laboratoire Ingénierie Circulation Transport LICIT (INRETS/ENTPE)*

---

## Abstract

A crucial challenge faced by current microscopic traffic flow models is capturing the relaxation phenomena commonly observed near congested on-ramps: vehicles are willing to accept very short spacings as they enter the freeway, but “relax” to more comfortable values shortly thereafter. This paper introduces a framework to solve this problem using a macroscopic theory of vehicle lane-changing inside microscopic models. In this theory, lane changes take place according to a stochastic process that has been validated in the field, and whose mean value is a function of lane-specific macroscopic quantities. As a consequence, the lane-changing logic becomes very simple compared to existing microscopic lane-changing models, and requires only one extra parameter. The resulting microscopic model is validated with empirical data.

*Key words:*

Lane-changing, microscopic traffic flow models, kinematic wave (LWR) model.

---

## 1 Introduction

Traditionally, the car-following component of traffic flow models has received much more attention than its lane-changing component. This is unfortunate because recent empirical evidence indicates that lane changing appears to be responsible for most traffic instabilities, such as capacity drop (Cassidy and Rudjanakanoknad, 2005) and the formation and propagation of stop-and-go

---

\* Corresponding author. Tel. : +1 (404) 894-2360; Fax : +1 (404) 894-2278  
*Email address:* [jorge.laval@ce.gatech.edu](mailto:jorge.laval@ce.gatech.edu) (Jorge A. Laval).

waves (Ahn and Cassidy, 2006). Moreover, a multilane hybrid (MH) theory (Laval and Daganzo, 2006) showed that the bounded acceleration of a lane change into a faster-moving lane can explain such instabilities at lane-drop and moving bottlenecks, and also at merge bottlenecks (Laval, 2007; Laval et al., 2007).

Interestingly, it was shown that the discretionary lane-changing rates on multilane freeways can be well approximated by a discrete-time function,  $\Phi(\cdot)$ , of macroscopic traffic flow variables (Laval and Daganzo, 2006; Laval et al., 2007). Here we show that  $\Phi(\cdot)$  has a continuum limit, which ensures consistency and well-posedness. It was also found in Laval and Daganzo (2006) that the speed of vehicles in the queue behind the disruptive lane changer obeys the moving bottlenecks (MB) model (Newell, 1993, 1998; Muñoz and Daganzo, 2002b; Leclercq et al., 2004). These results are important because it means that the complex lane-changing process can be predicted accurately with a parsimonious model that requires only one extra parameter; ie, the time to complete a lane-changing maneuver.

In contrast, current microscopic models base the lane-changing decisions on complex behavioral decision-making processes that require several (in some cases more than 30) parameters (eg, Gipps, 1986; Hidas, 2002, 2005; Wagner et al., 1997; Ahmed et al., 1996). These decision processes are typically evaluated at each time-step of the simulation, which may produce inconsistent and ill-posed models. This happens because the underlying discrete process is not derived from a continuum model. When this happens, the total number of lane changes depends on the number of times the decision-making process is evaluated inside the simulation; therefore, the duration of the time step becomes a parameter of the model, which result in models that do not converge to a continuum limit and therefore are inconsistent.

Additionally, the gap acceptance component of these models usually produces too few lane changes (see eg, Hidas, 2005), and causes what we call in this paper the *overreaction effect*. This latter effect arises when the spacings immediately after the lane change (between the subject vehicle and its leader and/or its follower on the target lane) are smaller than the fundamental diagram spacings associated with the speed on the target lane. In this situation car-following rules predict speeds far below the MB model, but more importantly far below empirical observations. To circumvent this problem current models introduce additional parameters to include courtesy and forced lane changes. The resulting large number of parameters and the necessity to assume the intentions of other vehicles adds complexity and instability to the overall process.

A crucial drawback of current microscopic lane-changing models is that they do not address the *relaxation phenomenon*, revealed empirically long ago by

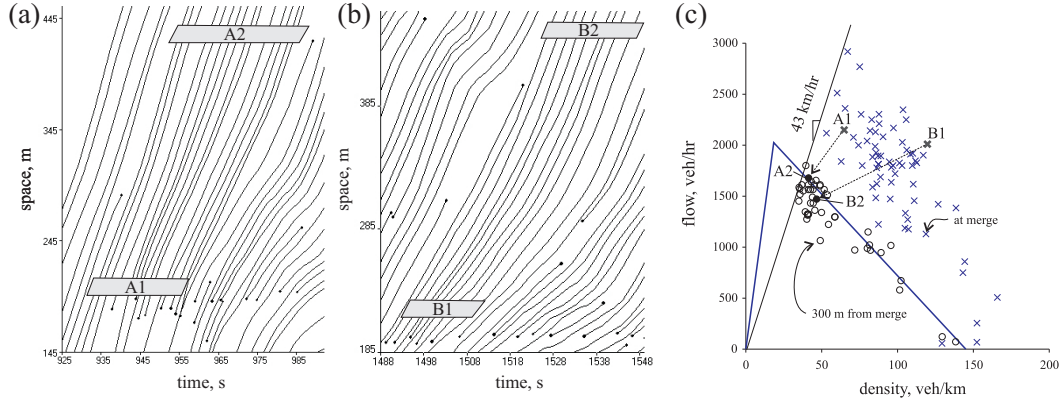


Fig. 1. (a)-(b) Trajectories taken from the NGSIM dataset for the shoulder lane in the vicinity of Powell St on-ramp on I-80 freeway in Berkeley, California; (c) flow-density measurements in this lane immediately downstream (crosses), and 300 m downstream (circles) of the on-ramp.

Smith (1985). He observed that vehicles involved in a lane-changing maneuver accept short spacings during the first 20 or 30 seconds, gradually attaining more comfortable spacings. Figures 1a-b show two such examples taken from the NGSIM dataset (NGSIM, 2006) for the shoulder lane in the vicinity of Powell St on-ramp on I-80 freeway in Berkeley, California. It can be seen how small spacings are accepted near the on-ramp, followed by a gradual relaxation into more comfortable values. Part c of the figure shows flow-density measurements in this lane immediately downstream of the on-ramp (crosses) and 300 m downstream (circles). These measurements were calculated using Edie’s method (Edie, 1961) for numerous regions similar to the shaded regions in parts a and b of the figure. These regions were chosen in order to be able to measure the same vehicles at both locations; ie, none of the vehicles changed lanes in between these two locations. It can be seen that measurements near the on-ramp are in “non-equilibrium” (ie, to the right of the fundamental diagram), but converge to “equilibrium” (ie, to the fundamental diagram) further downstream after approximately 30 seconds. To the authors’ knowledge only one publication proposes a formulation for its representation inside microscopic models (Cohen, 2004). In this reference the non-equilibrium spacing is relaxed linearly to the equilibrium value within a fixed time frame. Unfortunately, the same car-following rule is used with this modified spacing, and thus the overreaction problem persists.

The objective of this paper is twofold. First, we introduce a methodology for incorporating the macroscopic lane-changing model  $\Phi$  into microscopic models; second, we formulate a single-parameter model able to capture the relaxation phenomena. To accomplish the first objective we need the microscopic version of the MB model, which is also developed in this paper. In the same spirit as in the MH model, where a triangular flow-density diagram is assumed, we consider the CFL car-following rule (Daganzo, 2006), which is free of numer-

ical errors (Leclercq et al., 2007b). Notice, however, that the methodology proposed hereafter can be embedded in any car-following model.

This paper is organized as follows: §2 presents background material on the MH model and the CFL car-following rule, §3 formulates the macroscopic lane-changing model and the MB model in microscopic framework, as well as the relaxation model; and §4 validates the model with field data in Cassidy and Rudjanakanoknad (2005). Finally, §5 presents a discussion.

## 2 Background

### 2.1 Overview of the multilane hybrid (MH) model

This is a brief description of the MH model; for the details see Laval and Daganzo (2006). In the MH model each lane obeys the kinematic wave theory of Lighthill and Whitham (1955) and Richards (1956) with triangular fundamental diagram. For a highway with  $n$  lanes, the continuum formulation of the MH model is

$$\frac{\partial k_\ell}{\partial t} + \frac{\partial(k_\ell v_\ell)}{\partial x} = \sum_{\ell' \neq \ell} \Phi(k_{\ell'}, k_\ell) - \Phi(k_\ell, k_{\ell'}) \quad , \quad \ell = 1 \dots n, \quad (1)$$

where  $k_\ell(t, x)$  and  $v_\ell(k_\ell)$  give the density and speed in lane  $\ell$  at the time-space point  $(t, x)$ ;  $\Phi(k_\ell, k_{\ell'})$  is the one-directional lane-changing rate from lane  $\ell$  to lane  $\ell'$  (with  $\ell \neq \ell'$ ) in units of veh/time-distance. In this paper we call  $\Phi$  the macroscopic lane-changing model. It is a result of balancing a demand for lane-changing, a desired set of through flows and the available space capacity (supply) in the target lane. This competition mechanism was only presented in discrete form in Laval and Daganzo (2006); its continuum form will be derived later in §3.1.

Discretionary lane changes are assumed to be triggered by speed differences between adjacent lanes; ie, the fraction of vehicles per unit time,  $\pi$ , wishing to change from lane  $\ell$  to lane  $\ell'$  is given by

$$\pi(k_\ell, k_{\ell'}) = \frac{\max\{v_{\ell'} - v_\ell, 0\}}{u\tau} \quad , \quad \forall \ell, \forall \ell' \neq \ell, \quad (2)$$

where  $u$  is free-flow speed and  $\tau$  can be roughly interpreted as the time to execute a lane-change maneuver. As shown in Laval et al. (2007), mandatory lane changes can be included using

$$\pi(k_\ell, k_{\ell'}) = \frac{1}{\Delta t} \quad , \quad \forall \ell, \forall \ell' \neq \ell, \quad (3)$$

where  $\Delta t$  is the simulation time-step. The discrete lane-changing particles are generated according to a Poisson process with mean  $\Phi$ . Finally, these particles act as moving bottlenecks with realistic accelerations in the target lane as per the MB model.

## 2.2 The car-following linear (CFL) model

An exact car-following formulation of the kinematic wave theory with triangular fundamental diagram for a single lane was recently found (Daganzo, 2006). For a given lane with free-flow speed  $u$ , wave speed  $w$ , and jam density  $\kappa$ , the CFL model can be expressed as

$$x_{j+1,\ell}^i = \min\{x_{j\ell}^i + u\Delta t, x_{j\ell}^{i-1} - 1/\kappa\}, \quad (4)$$

where  $x_j^i$  is the position of vehicle  $i$  along lane  $\ell$  at time-step  $j$ . This scheme is free of numerical errors provided that

$$\Delta t = \frac{1}{w\kappa}, \quad (5)$$

which should be in the order of 1 sec for typical values of  $w$  and  $\kappa$ . Notice that (5) corresponds to Courant-Friedrichs-Lewy's stability condition in Lagrangian coordinates expressed as an equality (Leclercq, 2007).

## 3 Model formulation

This section presents the formulation of the macroscopic lane-changing model,  $\Phi$ , in microscopic framework, the MB model in microscopic framework and the relaxation model.

### 3.1 The macroscopic lane-changing model in microscopic framework

In order to use the macroscopic lane-changing model  $\Phi$  inside a microscopic model we need its continuum formulation in order to quantize it into vehicle units. Although the convergence results in Laval and Daganzo (2006) suggest that such limit exists,  $\Phi$  was only presented in discrete form. This model is based on the incremental-transfer (IT) principle (Daganzo, 1997), a discrete model, which prorates available capacity to the different demands following a FIFO rule. In the case of lane-changing Laval and Daganzo (2006) prorate the available capacity on the target lane to the different demands on the origin lanes.

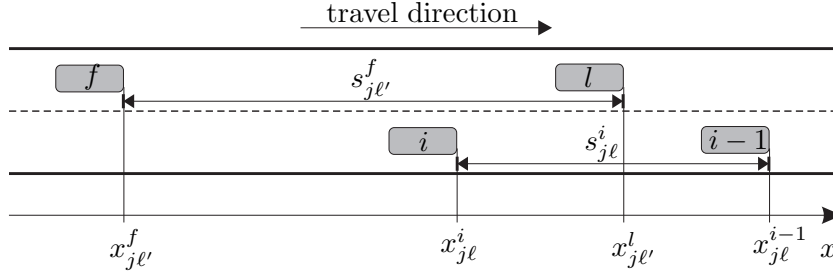


Fig. 2. Configuration prior to vehicle  $i$ 's lane change between new leader  $l$  and follower  $f$  on the target lane  $\ell'$ .

In order to find the continuum formulation for  $\Phi$  we take the limit of eqns. (5)-(13) in Laval and Daganzo (2006) as the mesh size tends to zero. This produces macroscopic lane-changing rates given by

$$\Phi(k_\ell, k_{\ell'}) = \min\left\{1, \frac{\mu(k_{\ell'})}{\lambda(k_{\ell'})}\right\} \frac{\pi(k_\ell, k_{\ell'})\lambda(k_\ell)}{u}, \quad (6)$$

where  $\lambda$  and  $\mu$  correspond to the demand (sending) and supply (receiving) functions of kinematic wave theory with triangular fundamental diagram, ie

$$\lambda(k) = \min\{uk, Q\}, \quad (7a)$$

$$\mu(k) = \min\{(\kappa - k)w, Q\}, \quad (7b)$$

where  $Q = uw\kappa/(u + w)$  is the one-lane capacity. The existence of the continuum limit (6) ensures that the lane-changing rates are physically well defined. In the microscopic framework, however, this continuum process needs to be quantized into vehicle units. Towards this end, let  $p_{\ell\ell'}^{ij}$  be the probability of vehicle  $i$  currently in lane  $\ell$  of switching to lane  $\ell'$  during time-step  $j$ . This probability can be interpreted as the integral of  $\Phi$  from  $t = t_j$  to  $t = t_{j+1}$  and over the spacing of vehicle  $i$  at time-step  $j$ ,  $s_{j\ell}^i = x_{j\ell}^{i-1} - x_{j\ell}^i$ . Assuming that  $\Phi$  varies slowly, we use the following approximation

$$p_{\ell\ell'}^{ij} = \int_{t=t_j}^{t_{j+1}} \int_{x=x_{j\ell}^i}^{x_{j\ell}^{i-1}} \Phi(k_\ell(t, x), k_{\ell'}(t, x)) dt dx \quad (8a)$$

$$\approx \Phi(k_\ell(t_j, x_{j\ell}^i), k_{\ell'}(t_j, x_{j\ell}^i)) \Delta t s_{j\ell}^i. \quad (8b)$$

Densities and spacings are related by

$$k_\ell(t_j, x_{j\ell}^i) = 1/s_{j\ell}^i, \quad (9a)$$

$$k_{\ell'}(t_j, x_{j\ell}^i) = 1/s_{j\ell'}^f, \quad (9b)$$

where  $f$  gives  $i$ 's new follower in the target lane  $\ell'$ ; see Fig. 2. Finally, lane changes are executed according to a Bernoulli process with probability of success  $p_{\ell\ell'}^{ij}$ , and are assumed to occur instantaneously.<sup>1</sup>

<sup>1</sup> Notice that a Bernoulli process converges to a Poisson process for small time-

### 3.2 The microscopic moving bottleneck (MB) model

Newell's MB model considers moving bottlenecks as pointwise moving boundary conditions; ie, with no physical dimension. Therefore, moving bottlenecks cannot be represented by regular cars obeying the CFL rule, as one would observe the overreaction effect presented in the introduction. This problem would arise whenever vehicle  $i$  changes lanes too close from its new leader  $l$  and/or  $f$  in Fig 2; in this case potential non-equilibrium vehicles are  $i$  and  $f$ . Hereafter, for clarity in notation we drop the lane-indices since we concentrate on a the target lane only, and we use  $i - 1 \equiv l$  and  $i + 1 \equiv f$ .

Let  $N(t, x)$  be the cumulative number of vehicles that have crossed location  $x$  by time  $t$  on the target lane under consideration, and let  $\Delta N_j^i$  be the difference in  $N$  between vehicle  $i$  and its leader  $i - 1$ ; ie,  $\Delta N_j^i = N(t_j, x_j^i) - N(t_j, x_j^{i-1})$ .

Of course, one would expect that  $\Delta N_j^i = 1$  always. However, since a moving bottleneck is treated here as a boundary condition without physical dimension one is forced to relax this assumption and allow for values  $\Delta N_j^i < 1$ . By doing this, one ensures full consistency with the continuum MB model. In fact, when vehicle  $j$  is in equilibrium  $\Delta N_j^i = 1$ ; otherwise,  $\Delta N_j^i < 1$ . Notice, however, that the difference in vehicle number between the moving bottleneck's leader and the moving bottleneck's follower always equals two, so that vehicles are conserved at all times; see Fig. 3b. Notice too that for the purposes of the MB model  $\Delta N_j^i$  is time-independent; but we keep the time index because it will be useful for the relaxation model formulation in the next section.

We will show that the car-following rule:

$$x_{j+1}^{i+1} = \min\left\{\underbrace{x_j^{i+1} + \min\{u, v_j^{i+1} + a\Delta t\}\Delta t}_{\text{free-flow term}}, \underbrace{x_j^i + v_{j+1}^i \Delta t - \frac{\Delta N_{j+1}^{i+1}}{K(v_{j+1}^i)}}_{\text{congestion term}}\right\}, \quad (10)$$

is the microscopic version of the MB model. The term  $K(v)$  gives the density in congestion associated with speed  $v$ , ie

$$K(v) = \frac{w\kappa}{v + w}, \quad (11)$$

and  $a$  is the desired acceleration of vehicle  $i + 1$ , which may be a function of vehicle type, current speed, grade, etc.

Car-following model (10) can be viewed as a generalization of the CFL model (4). The free-flow term incorporates bounded accelerations into the model, but is equivalent to the free-flow term in (4) by setting  $a = \infty$ . The congested

---

steps.

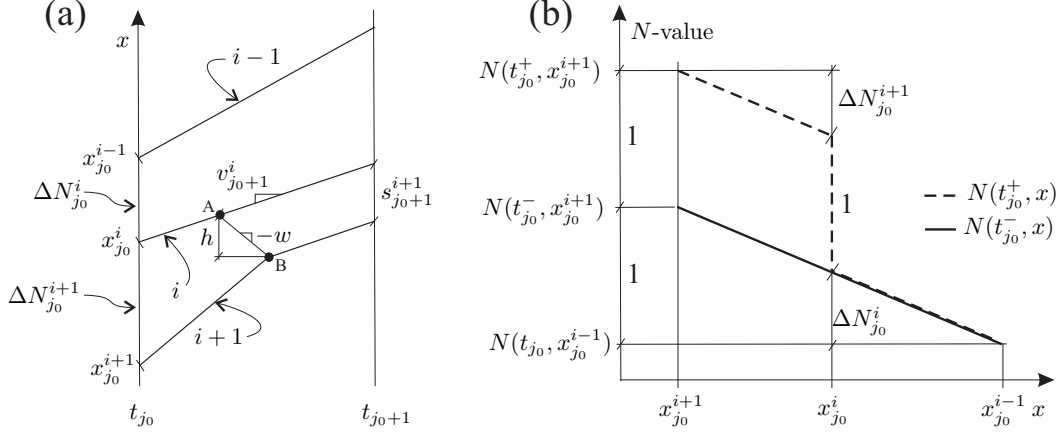


Fig. 3. (a) Time-space diagram during the time-step following the lane change of vehicle  $i$  between new leader  $i - 1$  and follower  $i + 1$  in the target lane; (b) evolution of  $N$  before and after the lane change.

term simplifies to  $x_j^i + v_{j+1}^i \Delta t - 1/K(v_{j+1}^i)$  when the follower is in equilibrium, ie when  $\Delta N_{j_0}^{i+1} = 1$ ; using (5) and (11) gives the congested term in (4) as sought. It follows that (10) can be used for all vehicles regardless of their equilibrium status. Notice that the term  $v_{j+1}^i$  in (10) implies that one has to update vehicle positions in the order of ascending  $i$ 's.

We now prove that the congested term in (10) follows from variational theory for kinematic wave problems (Daganzo, 2005). Figure 3a presents the time-space diagram during the time-step following the lane change of vehicle  $i$  at  $(t_{j_0}, x_{j_0}^i)$  between new leader  $i - 1$  and follower  $i + 1$  on the target lane. Without loss of generality, it is assumed that  $i$  causes a (moving) bottleneck and that  $i + 1$  is the only non-equilibrium vehicle; otherwise one may simply replace  $i$  by  $i - 1$  and  $i + 1$  by  $i$  in what follows.

Let B be the  $(t, x)$ -point where vehicle  $i + 1$  becomes constrained by  $i$ ; see Fig. 3a. Therefore, through line A-B pass  $h\kappa$  vehicles, where  $h$  is the distance traveled by the wave between  $i$  and  $i + 1$ . Since  $\Delta N_{j_0}^{i+1}$  is time-independent we have that  $\Delta N_{j_0}^{i+1} = \Delta N_{j_0+1}^{i+1} = h\kappa$ . From the geometry of this figure  $h$  also satisfies  $h = s_{j_0+1}^{i+1} w / (v_{j_0+1}^i + w)$ , and therefore

$$s_{j_0+1}^{i+1} = \frac{\Delta N_{j_0+1}^{i+1}}{K(v_{j_0+1}^i)}. \quad (12)$$

From Fig. 3a it is clear that  $x_{j_0+1}^{i+1} = x_{j_0}^i + v_{j_0+1}^i \Delta t - s_{j_0+1}^{i+1}$ . Hence, the congested term in (10) follows.

To determine  $\Delta N_{j_0}^i$  let  $t_{j_0}^-$  and  $t_{j_0}^+$  be the instants right before and after the lane change, respectively. Since the continuum MB model considers moving bottlenecks as moving boundary conditions, the  $N$ -profiles  $N(t_{j_0}^-, x)$  and  $N(t_{j_0}^+, x)$ ,  $x_{j_0}^{i+1} \leq x \leq x_{j_0}^{i-1}$ , remain unchanged in the continuum case. But in

our case the moving bottleneck is a vehicle and therefore introduces a discontinuity of unit magnitude to the  $N$ -profile. This is illustrated in Fig. 3b where the solid line corresponds to  $N(t_{j_0}^-, x)$  and the dashed line to  $N(t_{j_0}^+, x)$ . It can be seen that  $N(t_{j_0}^-, x)$  is a straight line of slope  $1/(x_{j_0}^{i-1} - x_{j_0}^{i+1})$  and that  $N(t_{j_0}^+, x)$  is similar but exhibits a jump of unit magnitude at  $(t_{j_0}, x_{j_0}^i)$ . However, it becomes clear from the figure that the difference in vehicle number between  $i$  and its neighbors remains single-valued and equal to

$$\Delta N_{j_0}^i = \frac{x_{j_0}^{i-1} - x_{j_0}^i}{x_{j_0}^{i-1} - x_{j_0}^{i+1}} \quad \text{and} \quad \Delta N_{j_0}^{i+1} = \frac{x_{j_0}^i - x_{j_0}^{i+1}}{x_{j_0}^{i-1} - x_{j_0}^{i+1}} \quad (13)$$

as illustrated in Fig. 3b. This definition is consistent with the initial conditions of the problem; ie, the initial density surrounding the bottleneck is  $(x_{j_0}^{i-1} - x_{j_0}^{i+1})^{-1}$ .

Notice that the proposed model places no restrictions to the spacings  $x_{j_0}^{i-1} - x_{j_0}^i$  and  $x_{j_0}^i - x_{j_0}^{i+1}$ . Therefore, short spacings may be generated and may appear unrealistic at the microscopic level. However, this ensures that lane-changing rates given by (6) are respected, and guaranties consistency at the macroscopic level. Moreover, the short spacings created by the model are only transient thanks to the relaxation procedure proposed next, whose main objective is to incorporate the driver behavior discussed in Fig. 1.

### 3.3 The relaxation model

The goal of the relaxation procedure is to have non-equilibrium vehicles gradually adapt to the CFL model. This can be accomplished in several ways with different levels of complexity. Here we propose a method that requires a single observable parameter, the relaxation speed-gap,  $\varepsilon$ . Fig. 4a depicts the follower and bottleneck trajectories in time-space from the time-step following the lane change, ie from  $j = j_0 + 1$ . Without loss of generality we assumed in the figure that the bottleneck accelerates, so that  $v_{j+2}^i > v_{j+1}^i$ . It is clear that once  $v_{j+1}^{i+1}$  is known the follower spacing obeys

$$s_{j+1}^{i+1} = s_j^{i+1} + (v_{j+1}^i - v_{j+1}^{i+1})\Delta t. \quad (14)$$

We note that for  $j > j_0$  differences in vehicle number and spacings are related by (12), ie

$$\Delta N_j^{i+1} = s_j^{i+1} K(v_j^i) \quad \text{with} \quad j > j_0. \quad (15)$$

Combining (14)-(15) gives the following updating scheme

$$\Delta N_{j+1}^{i+1} = \left[ \frac{\Delta N_j^{i+1}}{K(v_j^i)} + (v_{j+1}^i - \tilde{v}_{j+1}^{i+1})\Delta t \right] K(v_{j+1}^i), \quad (16)$$

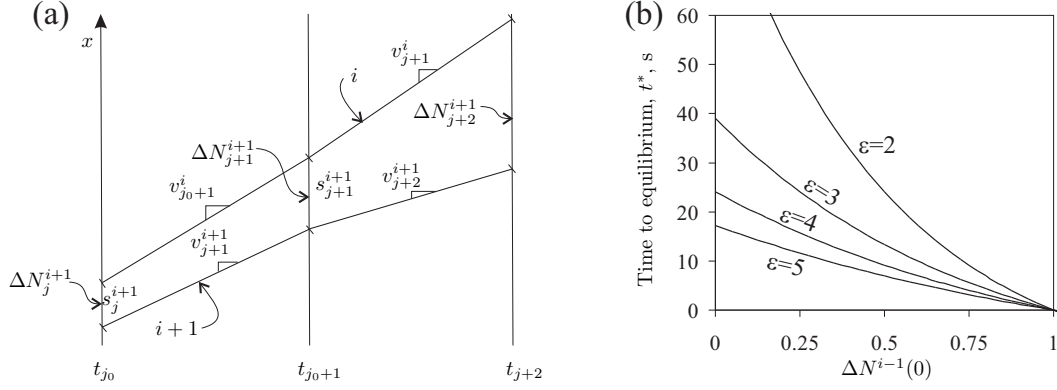


Fig. 4. (a) Time-space diagram showing the follower and bottleneck trajectories from the time-step following the lane change (from  $j = j_0 + 1$ ); (b) time to convergence to equilibrium as a function of  $\Delta N^{i+1}(0)$  for different values of  $\epsilon$  assuming  $w = 22$  km/h,  $\kappa = 150$  veh/km,  $\beta = 1$  m/s<sup>2</sup> and  $v^i(0) = 30$  km/hr.

where we have introduced the follower's desired speed,  $\tilde{v}_{j+1}^{i+1}$ , since its actual speed  $v_{j+1}^{i+1}$  is not known at this stage. In this paper we propose the following expression for desired speeds

$$\tilde{v}_{j+1}^{i+1} = \underbrace{v_{j+1}^i(1 - \Delta N_j^{i+1}) + v_j^i \Delta N_j^{i+1}}_{\text{MB-speed}} - \epsilon. \quad (17)$$

When  $\epsilon = 0$ ,  $\tilde{v}_{j+1}^{i+1}$  is given by the speed predicted by the MB model without relaxation; this speed can be obtained by setting  $\Delta N_{j+1}^{i+1} = \Delta N_j^{i+1}$  in (16) and solving for  $\tilde{v}_{j+1}^{i+1}$ . It can be seen that the MB-speed is a convex combination of  $v_j^i$  and  $v_{j+1}^i$ : when  $i + 1$  is close to  $i$  then  $\Delta N_j^{i+1}$  is small and the MB-speed is close to  $v_{j+1}^i$ ; otherwise, when  $i + 1$  is far from  $i$  the MB-speed is close to  $v_j^i$ . It follows that  $\epsilon$  can be interpreted as the speed difference the follower is willing to accept with respect to its leader in order to attain an equilibrium spacing.

To make sure this procedure is physically well defined, one can compute its continuum limit, ie the difference in vehicle number by time  $t$ ,  $\Delta N^{i+1}(t)$ . To this end, we obtain its time derivative by computing  $(\Delta N_{j+1}^{i+1} - \Delta N_j^{i+1})/\Delta t$  using (16)-(17) and letting  $\Delta t$  go to zero. This gives the ODE

$$\frac{d}{dt} \Delta N^{i+1}(t) = \epsilon K(v^i(t)), \quad (18)$$

where  $v^i(t)$  is the speed of vehicle  $i$  at time  $t$ . This expression indicates that  $\Delta N^{i+1}(t)$  grows proportionally to  $\epsilon$ , as expected, but inversely proportional to  $v^i(t)$ —due to (11)—which may be somewhat surprising. In fact, as the bottleneck travels faster the equilibrium spacing grows and therefore it would take longer to reach equilibrium. For illustration purposes, we measure time starting at  $t = t_{j_0+1} = 0$  and imagine that the bottleneck adopts a constant ac-

celeration rate  $\beta > 0$ , ie  $v^i(t) = v^i(0) + \beta t$ . Solving (18) with initial conditions  $\Delta N^{i+1}(0)$  gives

$$\Delta N^{i+1}(t) = \Delta N^{i+1}(0) + \frac{\varepsilon w \kappa}{\beta} \ln \left[ 1 + \frac{\beta t}{v^i(0) + w} \right], \quad (19)$$

which reveals that  $\Delta N^{i+1}(t)$  grows logarithmically in time. This guarantees that the time to convergence to equilibrium,  $t^*$ , is finite; moreover, it equals

$$t^* = \frac{v^i(0) + w}{\beta} \left( \exp \left[ \beta \frac{1 - \Delta N^{i+1}(0)}{\varepsilon w \kappa} \right] - 1 \right). \quad (20)$$

Fig. 4b shows  $t^*$  as a function of  $\Delta N^{i+1}(0)$  for  $\beta = 1 \text{ m/s}^2$  and  $v^i(0) = 30 \text{ km/hr}$ . Considering that the average value for  $\Delta N^{i+1}(0)$  in our model should be close to 0.5, it can be seen that  $\varepsilon \approx 2 \text{ km/hr}$  yields times to equilibrium in the order of 30 seconds, which is consistent with observations; see Figs. 1a-b.

#### 4 Model validation

In this section we validate the proposed model with the empirical observations recorded in October 21st, 2003 by Cassidy and Rudjanakanoknad (2005) at an on-ramp merge bottleneck; see sketch in Fig. 5a. These are the first high-resolution experiments to reveal capacity drops and recoveries due to varying ramp metering strategies. They found that (i) the capacity drop occurs simultaneously with an increase in lane-changing counts and shoulder lane vehicle accumulation, and that (ii) controlling the ramp-metering rate could mitigate this lane changing and accumulation, so that high merge capacities could be restored. They manually extracted from videos the following traffic data: (i)  $N(t)$ -curves measured at the four locations labelled  $X_1$  through  $X_4$  in Fig. 5a; (ii) vehicle accumulations in the shoulder lane between  $X_1$  and  $X_3$ ; and (iii) cumulative number of lane changes leaving the two rightmost lanes between  $X_1$  and  $X_3$ ,  $LC(t)$ . Notice that this latter curve does not consider the incoming on-ramp flow as lane-changes.

For the simulations we used the model parameters suggested in Laval et al. (2007):  $u = 112 \text{ km/h}$ ,  $w = 22 \text{ km/h}$  and  $\tau = 4 \text{ sec}$ ; here we found that  $\kappa = 150 \text{ veh/km}$  and  $\varepsilon = 2 \text{ km/hr}$  produce adequate fit. As in Laval et al. (2007), for the acceleration capabilities of lane-changing vehicles we chose the vehicle kinetics model in McLean (1989) for an average car on level terrain:  $a(v) = 3.4(1 - v/123.8) \text{ m/s}^2$ , where the numbers  $3.4 \text{ m/s}^2$ , and  $123.8 \text{ km/hr}$  correspond to the maximum acceleration and maximum speed, respectively. The input data consisted of the lane-specific traffic demands measured in 30-sec intervals at a loop-detector located upstream of  $X_1$ , while on-ramp demand was taken from Cassidy and Rudjanakanoknad (2005). The length of

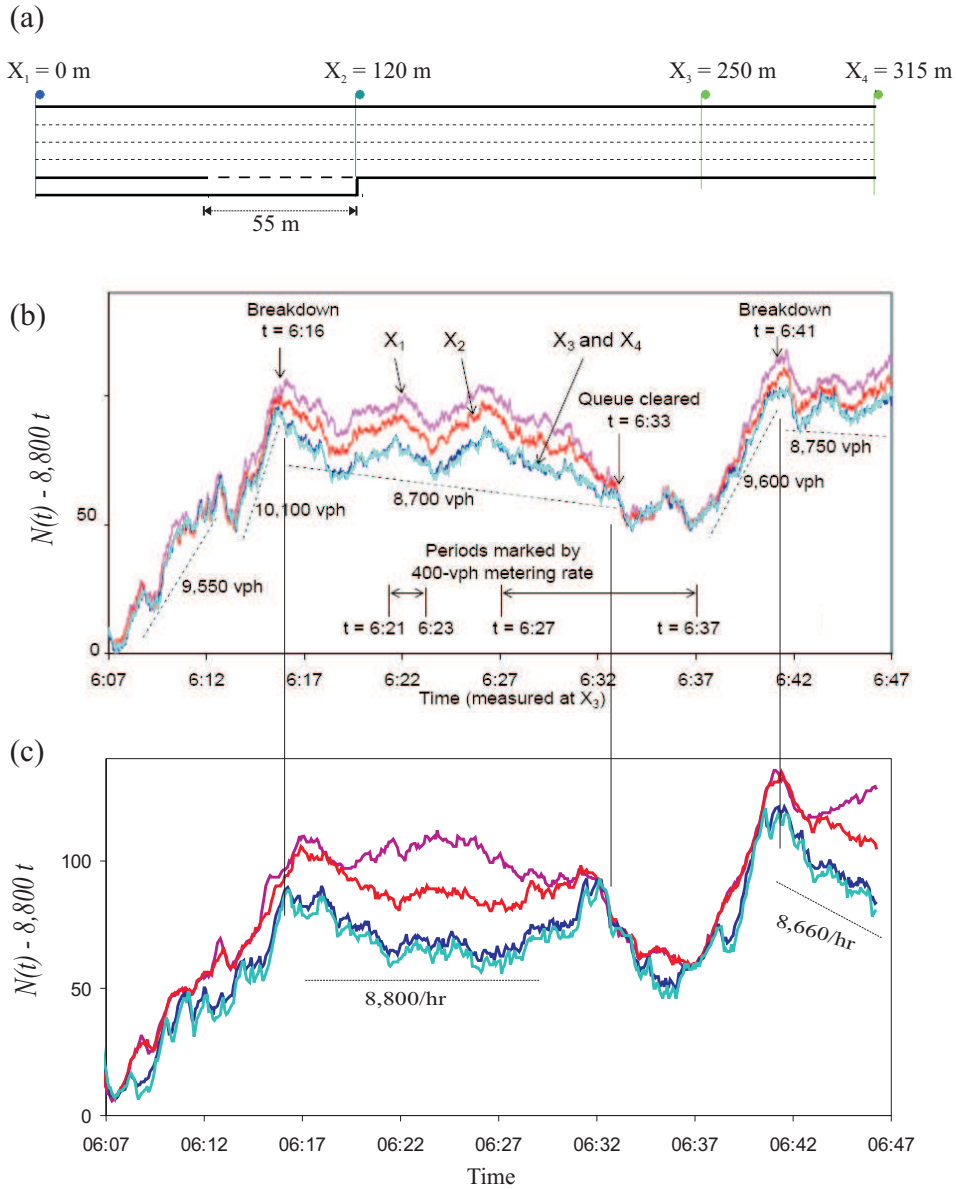


Fig. 5. (a) Site sketch; oblique queuing diagrams: (b) measured (taken from Cassidy and Rudjanakanoknad, 2005); (c) simulated.

the merging area was estimated to be 55 m from satellite imagery; see Fig. 5a. lane changes inside this section are considered mandatory; ie, as per (3).

Simulation results are shown below the corresponding empirical charts in Figs. 5 and 6. Vertical solid lines connecting the empirical and simulated charts have been added to facilitate comparisons. Notice that the curves  $N(t) - 8800t$  are oblique cumulative plots (Muñoz and Daganzo, 2002a), where a background flow of 8,800 vph is subtracted in order to magnify the changes in the cumulative curves. It can be seen from Fig. 5 that the simulation accurately predicts bottleneck activation times (to within 30 seconds of the observed times) and bottleneck discharge rates (to within 1%).

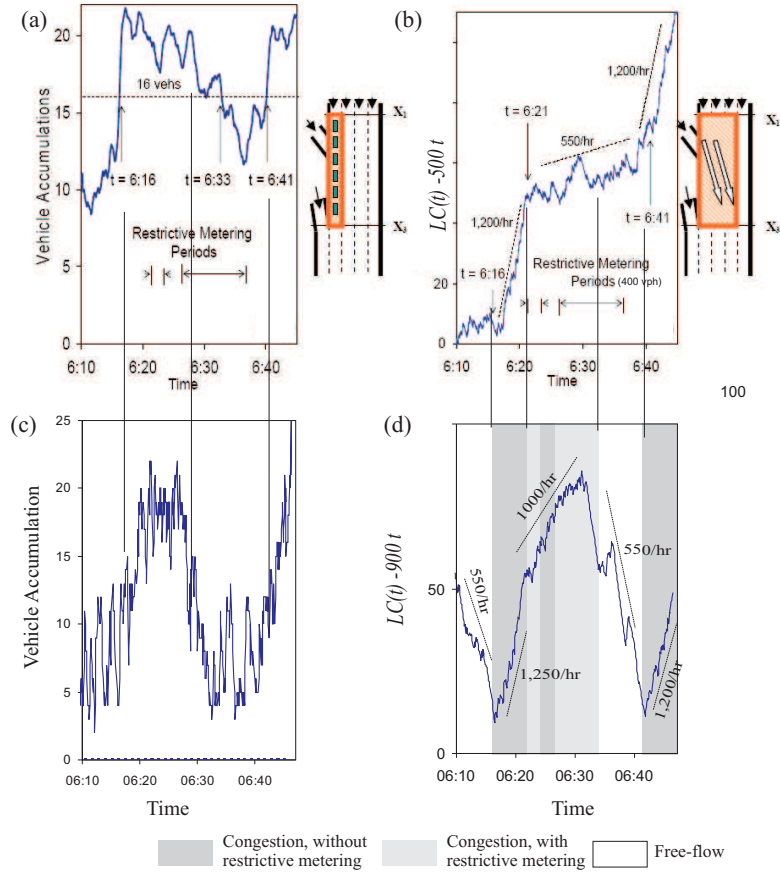


Fig. 6. Time series of accumulations and lane-changing: (a) measured shoulder lane accumulation; (b) measured lane-changing flows; (c) simulated shoulder lane accumulation; (d) simulated lane-changing flows. (Parts a and b were taken from Cassidy and Rudjanakanoknad, 2005).

The key features of shoulder-lane accumulations and cumulative lane changes (Fig. 6) are also reproduced by the theory. In particular, the predicted time series of shoulder-lane accumulations exhibits similar shapes to those observed, though the theory underpredicts the numeric values during free-flow conditions. Predicted lane-changing maneuvers match those observed during free-flow and also during congested times outside of restrictive metering periods (this traffic regime is color-coded dark gray in Fig. 6d). Prediction errors arise only for the first period of congestion during restrictive metering periods (light gray in the figure). Notably, the observed times of regime change are also closely matched by the theory.

## 5 Discussion

This paper introduced a framework for incorporating a macroscopic theory of vehicle lane-changing rates into microscopic models. In this theory, lane

changes take place according to a stochastic process that has been validated in the field, and whose mean value is a function of lane-specific macroscopic quantities. As a consequence, the lane-changing logic becomes very simple compared to existing microscopic lane-changing models, and requires only one extra parameter. Additionally, the proposed framework allowed us to postulate a model to capture the relaxation phenomena that often takes place after a lane change. The results are appealing especially in light of the good fit with the macroscopic empirical data presented in this paper.

A sequel to this paper (Leclercq et al., 2007a) has validated the relaxation model proposed herein with the microscopic data from NGSIM, and shows that the relaxation phenomena cannot be ignored near congested on-ramps. One can conclude that the logarithmic relaxation process unveiled by (19) is in fact realistic. In terms of the spacing, one can combine (19) and (15), which gives

$$s^{i+1}(t) = (1 + c_1 t)(s^{i+1}(0) + c_2 \ln(1 + c_1 t)), \quad (21)$$

with  $c_1 = \beta/(v^i(0) + w)$  and  $c_2 = \varepsilon(v^i(0) + w)/\beta$ . Reassuringly, one can verify that the functional form suggested by (21) is consistent with other published microscopic data (eg, Figs. 2 and 7 in Hidas, 2005). This expression also highlights the influence of the leader's acceleration,  $\beta$ , in the relaxation process.

This paper also showed the existence of a continuum lane-changing rate function (6), which can be useful for solving the multilane kinematic wave model (1) using variational theory (Daganzo, 2005). In particular, the number of lane changes through an arbitrary path in time-space can be obtained by integrating (6) along this path. Result (6) could also be used for deriving closed-form capacity formulae on bottlenecks caused by the presence of slow vehicles. To do this one should approximate lane change trajectories by piecewise-linear ones so that the stochastic process becomes a renewal process, following the framework in Laval (2006).

It is worth stressing that the trajectories resulting from the proposed microscopic model need to be interpreted with care since this model is conceptually different from existing microscopic models. In particular, it is possible to find arbitrarily short (non-equilibrium) spacings following a lane change, which could seem “unrealistic”. This is a result of (i) using a macroscopic lane-changing model, and (ii) assuming that lane changes occur instantaneously. However, the latter assumption is needed only for the numerical solution method, which leaves room for alternative physical interpretation. For example, non-equilibrium spacings should be interpreted as such once the lane-changing maneuver has been completed (ie, after  $\tau$  time units following the lane change), in which case spacings tend to be more “realistic”. Under this understanding, our driver experience tells us that it is indeed possible to

see very short spacings, especially at the beginning of the maneuver when the lane-changing vehicle is still in its origin lane.

It was mentioned in §3.1 that the car-following model (10) has to be updated in the order of ascending  $i$ 's, which may be disadvantageous for engineering applications on large-scale networks. It is possible to avoid this sequential updating at the expense of extra memory requirements, or at the expense of numerical errors. One may use the method described in Leclercq et al. (2007b) which requires keeping in memory the state of the system in two consecutive time steps, rather than in a single time step with the model presented here. Another possibility is to use an approximation of  $v_{j+1}^{i-1}$  (eg,  $v_j^{i-1}$  or some other “anticipation speed”), but this would introduce numerical errors with respect to the continuum MB model.

## References

- Ahmed, K., Ben-akiva, M., Koutsopoulos, H., Mishalani, R., 1996. Models of freeway lane changing and gap acceptance behavior. In: Lesort, J. B. (Ed.), 13th Int. Symp. on Transportation and Traffic Theory. Elsevier, New York.
- Ahn, S., Cassidy, M., 2006. Freeway traffic oscillations and vehicle lane-change manoeuvres. In: Heydecker, B., Bell, M., Allsop, R. (Eds.), Forthcoming in 17th International Symposium on Transportation and Traffic Theory. Elsevier, New York.
- Cassidy, M., Rudjanakanoknad, J., 2005. Increasing capacity of an isolated merge by metering its on-ramp. *Transportation Research Part B* 39 (10), 896–913.
- Cohen, S. L., 2004. Application of relaxation procedure for lane changing in microscopic simulation models. *Transportation Research Record* 1883, 50–58.
- Daganzo, C. F., 1997. A continuum theory of traffic dynamics for freeways with special lanes. *Transportation Research Part B* 31 (2), 83–102.
- Daganzo, C. F., 2005. A variational formulation of kinematic waves: Basic theory and complex boundary conditions. *Transportation Research Part B* 39 (2), 187–196.
- Daganzo, C. F., 2006. In traffic flow, cellular automata = kinematic waves. *Transportation Research Part B* 40 (5), 396–403.
- Edie, L. C., 1961. Car following and steady-state theory for non-congested traffic. *Operations Research* 9, 66–77.
- Gipps, P. G., 1986. Multsim: a model for simulating vehicular traffic on multi-lane arterial roads. *Mathematics and Computers in Simulation* 28 (4), 291–295.
- Hidas, P., 2002. Modelling lane changing and merging in microscopic traffic simulation. *Transportation Research Part C* 10 (5-6), 351–371.

- Hidas, P., 2005. Modelling vehicle interactions in microscopic simulation of merging and weaving. *Transportation Research Part C* 13, 37–62.
- Laval, J. A., 2006. Stochastic processes of moving bottlenecks: Approximate formulas for highway capacity. *Transportation Research Record* 1988, 86–91.
- Laval, J. A., 2007. Linking synchronized flow and kinematic wave theory. In: Kuhne, R., Poschel, T., Schadschneider, A., Schreckenberg, M., Wolf, D. (Eds.), *Traffic and Granular Flow'05* (In Press). Springer.
- Laval, J. A., Cassidy, M. J., Daganzo, C. F., 2007. Impacts of lane changes at on-ramp bottlenecks: A theory and strategies to maximize capacity. In: Kuhne, R., Poschel, T., Schadschneider, A., Schreckenberg, M., Wolf, D. (Eds.), *Traffic and Granular Flow'05* (In Press). Springer.
- Laval, J. A., Daganzo, C. F., 2006. Lane-changing in traffic streams. *Transportation Research Part B* 40 (3), 251–264.
- Leclercq, L., 2007. Hybrid approaches to the solutions of the LWR model. *Transportation Research Part B* (in Press).
- Leclercq, L., Chanut, S., Lesort, J., 2004. Moving bottlenecks in the LWR model : a unified theory. *Transportation Research Record* 1883, 3–13.
- Leclercq, L., Chiabaut, N., Laval, J., Buisson, C., 2007a. Relaxation phenomenon after changing lanes: Experimental validation with NGSIM data set. *Transportation Research Record* (Forthcoming). Preprint available in the Transportation Research Board 2007 Annual Meeting CD-ROM.
- Leclercq, L., Laval, J., Chevallier, E., 2007b. The Lagrangian coordinate system and what it means for first order traffic flow models. In: Heydecker, B., Bell, M., Allsop, R. (Eds.), *Forthcoming in 17th International Symposium on Transportation and Traffic Theory*. Elsevier, New York.
- Lighthill, M. J., Whitham, G., 1955. On kinematic waves. I Flow movement in long rivers. II A theory of traffic flow on long crowded roads. *Proc. Roy. Soc.* 229 (A), 281–345.
- McLean, J. R., 1989. Two-lane highway traffic operations (TWOPAS). In: Ashford, N., Bell, W. (Eds.), *Transportation Studies*. Vol. 11. Gordon and Breach Science Publishers, Amsterdam.
- Muñoz, J., Daganzo, C. F., 2002a. Fingerprinting traffic from static freeway sensors. *Cooperative Transportation Dynamics* 1, 1.1–1.11.  
URL <http://vwitme011.vkw.tu-dresden.de/TrafficForum>
- Muñoz, J., Daganzo, C. F., 2002b. Moving bottlenecks: a theory grounded on experimental observation. In: Taylor, M. (Ed.), *15th Int. Symp. on Transportation and Traffic Theory*. Pergamon-Elsevier, Oxford, U.K., pp. 441–462.
- Newell, G. F., 1993. A simplified theory of kinematic waves in highway traffic, I general theory, II queuing at freeway bottlenecks, III multi-destination flows. *Transportation Research Part B* 27 (4), 281–313.
- Newell, G. F., 1998. A moving bottleneck. *Transportation Research Part B* 32 (8), 531–537.
- NGSIM, 2006. Next generation simulation.  
URL <http://ngsim.fhwa.dot.gov/>
- Richards, P. I., 1956. Shockwaves on the highway. *Operations Research* (4),

42–51.

Smith, S. A., 1985. Freeway data collection for studying vehicle interaction. Tech. Rep. FHWA/RD-85/108, FHWA, U.S., Department of Transportation.

Wagner, P., Nagel, K., Wolf, D., 1997. Realistic multi-lane traffic rules for cellular automata. *Physica A* 234 (3-4), 687–698.